J Nanotechnol Nanomaterials. 2026;7(1):28–39.

Journal of Nanotechnology and Nanomaterials Original Research

Investigation on Carbon Dot–Like Nanohybrids for Fluorescence Sensing of 2,4–Dinitrotoluene with Excitation at Multiple Visible Wavelengths

Kirkland Sheriff[1,*], Buta Singh[1], Simran Dumra[1], Subhadra Yerra[1], Jordan Collins[1], Ya–Ping Sun[1,*]

[1]Department of Chemistry, Clemson University, Clemson, SC 29634, USA

[*]Correspondence should be addressed to Kirkland Sheriff, ksherif@clemson.edu; Ya–Ping Sun, syaping@clemson.edu

Received date: August 31, 2026, **Accepted date:** October 13, 2026

Citation: Sheriff K, Singh B, Dumra S, Yerra S, Collins J, Sun YP. Investigation on Carbon Dot–Like Nanohybrids for Fluorescence Sensing of 2,4–Dinitrotoluene with Excitation at Multiple Visible Wavelengths. J Nanotechnol Nanomaterials. 2026;7(1):28–39.

Copyright: © 2026 Sheriff K, et al. This is an open-access article distributed under the terms of the Creative Commons Attribution License, which permits unrestricted use, distribution, and reproduction in any medium, provided the original author and source are credited.

Abstract

Carbon dots (CDots) and their related materials (namely nano–carbon/organic hybrids, or simply hybrids) are a class of nanomaterials with a variety of applications and have rich structural variability. Herein, the fluorescent hybrid materials were investigated for their ability to sense 2,4–dinitrotoluene (DNT) across multiple excitation wavelengths in the visible spectrum. The results show great sensitivity, especially at lower concentrations, for sensing DNT across the wavelengths investigated. Two precursor mixtures were employed for the thermal carbonization production of nano–carbon/organic hybrids, one using polyethylenimine (PEI) and citric acid (CA) and the other using diethylenetriamine (DETA) and CA. The two resulting samples were investigated for their sensing capabilities and shared characteristics: quenching constants of at least 41 M^{-1} and an order of magnitude higher at low DNT concentrations (measurements went as low as 2.5 x 10^{-5} M) and the excitation wavelength dependance. These results suggest that the hybrids are structurally more complex, with different sensing capabilities from those of the classically defined and synthesized CDots.

Keywords: Carbon dots, Nano–carbon/Organic hybrids, Fluorescence sensing, Nitroaromatics, Nanomaterials

Introduction

Carbon dots (CDots) [1–4] have generated much attention for a variety of applications and properties [5–7]. The most common property that has been explored, and justifiably so, has been the bright and colorful fluorescence [1,8,9] that is excitation wavelength dependent rather than size dependent as seen in classical quantum dots [3]. In addition to the colorful fluorescence, CDots can have very high fluorescence quantum yields, that may be close to unity in some cases [10–12]. The source of the fluorescence has been debated, but the leading theory is that the surface of a small carbon nanoparticle (CNP), <10 nm in diameter, acts as a core and has abundant surface sites that may be passivated [13–15] When photoexcitation in the core CNP occurs there is a rapid charge separation and migration to the surface sites. When there is a proper passivation of these surface sites there may be a suppression of non–radiative pathways which can facilitate radiative recombination of the charge carriers, resulting in fluorescence emission [3].

CDots were originally synthesized by harvesting carbon soot from laser ablation of graphite [1,16]. Since that original report in 2006 there have been many avenues explored for synthesis of CDots including soot harvesting from engines [17,18], coal [19], and candles [20], pyrolysis of small molecules using high temperature [21–23], and microwave assisted processing [24,25]. The pyrolysis of small molecules, whether from thermal means or using microwave assisted means, is the most common in literature due to its ease of production and low cost starting materials. The resulting materials from these techniques are typically more hybrid in nature in that there is not a sufficient carbonization of the precursors to produce a classically defined CNP core, see **Figure 1** [26–28]. As shown by Wang et al., the structure could be considered as more porous in nature when synthesized at lower temperature, therefore the authors suggested referring to those nanomaterials as nano–carbon/organic hybrids [4,29,30].

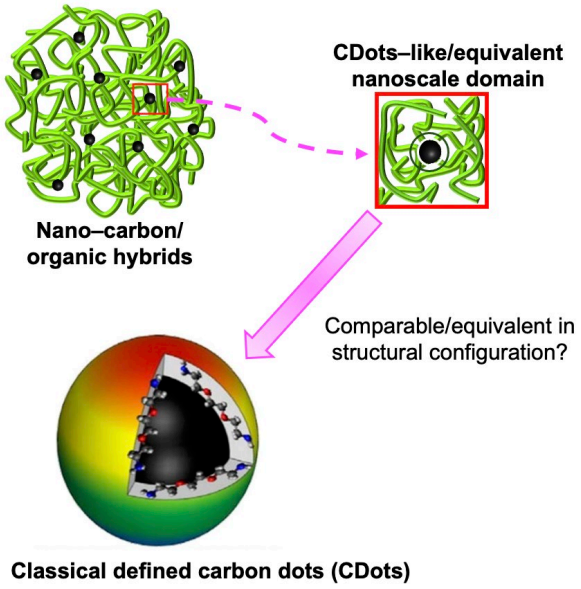


Figure 1. Illustration of carbon dot–like sample.

The applications of CDots are quite extensive, ranging from bioimaging [31,32], catalysis [33,34] to sensing [35–39]. Fluorescence sensing using CDots and nano–carbon/organic hybrids has been popular as a probe for a broad array of targeted analytes including metals, biomarkers, and explosives [24,40–42], with the detection limit well into the µM range (for example, the sensing of Hg^{2+} down to less than 0.02 µM) [24]. In particular, the sensing of nitroaromatic compounds is of great concern for security applications, due to their potential use in illicit activity [43]. It has been suggested that amine rich entities may interact more strongly with nitroaromatics (possibly through an Meisenheimer complex) [44,45], therefore, having a probe that contains ample amine groups may enhance the materials' ability to probe nitroaromatics presence. Often the sensing is accomplished with "turn–off" fluorescence, where the quencher can interact with emissive species more directly, though other and more complex mechanisms may exist [37]. The ability of CDots and nano–carbon/organic hybrids to sense hazardous materials extends beyond their application possibilities and into the structural aspect. As previously mentioned, Wang et al. deduced structural information using Cu^{2+} as a quencher and suggested that the hybrids had a great deal of porosity associated them [29]. The porous dot sample structure could be exploited for much enhanced sensitivity in fluorescence sensing by taking advantage of the significant static quenching associated with higher than bulk local concentrations of the sensing target.

The work reported here was to exploit the dot sample structural characteristics and the associated high sensing capabilities. Specifically, we used nano–carbon/organic hybrids produced using a microwave assisted method with different precursors to sense 2,4–dinitrotoluene (DNT). Varying the precursors alters the synthesis protocol slightly but the resulting materials have some similarities: a porous and optically active material. The use of these fluorescent CDots–like entities to sense hazardous materials such as nitroaromatics using longer excitation wavelengths in the visible spectrum is explored as well as the structural ramifications from the sensor materials processing technique are discussed herein.

Experimental Section

Materials

All reagents were used as received without additional purification. Citric acid (100%) was purchased from Viva Doria, diethylenetriamine (DETA, >99%) was purchased from Fischer Scientific, polyethylenimine (PEI, ≥99%, MW 1200 g/mol) was purchased from Polysciences, 2,4–dinitrotoluene (≥99.0%) was purchased from TCI America, methanol (99.85%) was purchased from Duda Energy, and ethanol (100%) was purchased from Pharmco.

Measurements

UV/Vis absorption spectra were collected on a Shimadzu UV–1280 and the fluorescence measurements were performed on a Shimadzu RF–6000 fluorimeter with a 150 W xenon arc lamp. Fluorescence quantum yields (Φ_F) were determined by using the relative method with 9,10–bis(phenylethynyl)–anthracene (BPEA) in hexanes and rhodamine 6G in ethanol as standards.

DETA/CA

Diethylenetriamine (DETA, 1 g) and citric acid (CA, 1 g) were mixed in water (2 mL) in a small scintillation vial (20 mL) and sonicated for 10 minutes, followed by the removal of the water *via* purging with nitrogen gas. Then the vial containing the sample mixture was immersed into a solid–state bath of silicon carbide (SiC) powder (150 g) in a silica crucible casting dish for the heating in a conventional microwave oven at the power of 100 W for 1 minute and 700 W for 4 minutes. The sample was cooled to ambient temperature and dispersed in water (10 mL) with sonication for 15 minutes, and the dispersion was centrifuged at 500 rpm (1,400 *g*) for 20 minutes to collect the supernatant. The solution of the as–prepared sample was dialyzed in membrane tubing (molecular weight cut–off ~1000) against fresh water for 2 hours to obtain aqueous solution of the DETA/CA hybrids.

PEI_{1200}/CA

Similar to work outlined in Singh et al. [46] and Hou et al. [47], polyethyleneimine PEI (M.W. 1200) (1 g) and citric acid (CA, 0.3 g) were mixed in water (1 mL) in a small scintillation vial, followed by the removal of the water *via* purging with nitrogen gas. Separately, a silica crucible casting dish containing silicon carbide (150 g) was pre–heated in a conventional microwave oven at 500 W for 3 minutes. The small scintillation vial (20 mL) containing the PEI and CA mixture was immersed in the pre–heated SiC bath for processing in a conventional microwave oven. The initial treatment was at 200 W for about 4 minutes until no bubbles were observed in the precursor sample and the sample color turned dark orange and then this initially prepared samples were further treated with microwave heating for 4 minutes at 700 W, with the resulting samples denoted as PEI_{1200}/CA. Post–treatment, the reaction mixture was cooled to ambient temperature and dispersed in ethanol. The solution of the as–prepared samples were dialyzed in membrane tubing (molecular weight cut–off ~1000) against fresh water for 24 hours to obtain aqueous solutions of the dot samples.

Sensing experimental details

The fluorescence sensing experiments were performed by preparing stock solutions of DNT in differing concentrations and adding them to a solution of the nano–carbon/organic hybrids. The quantum yield was subsequently determined and for each concentration of DNT added. The optical density of the nano–carbon/organic hybrids maintained at ~0.1. The range of the data collected was 0.0 M DNT to 5.0×10^{-2} M DNT. The nano–carbon/organic hybrids were dispersed in methanol for DETA/CA and ethanol for PEI_{1200}/CA. The DNT mother solutions were prepared in methanol for DETA/CA sensing and ethanol for PEI_{1200}/CA sensing. The quenching constants were determined using the equation: $\Phi_F^0/\Phi_F = 1 + K_{SV}[DNT]_{LOCAL}$.

Results and Discussion

Carbonizing small molecule precursors for production of nanoscale carbon is a simple route for producing carbon dot–like entities. Commercially available microwave ovens have long been employed, with great success [46,48–50], at making nanoscale carbon dot–like hybrids. These hybrids lack the well–defined carbon core (unlike the core carbon nanoparticles in the classically defined and synthesized carbon dots), but rather contain regions of nanoscale carbon interconnected via organic entities. This resulting material yields absorption and fluorescence emission spectra that may be similar to those of classical carbon dots (**Figure 2**). The hybrid materials may also exhibit characteristics such as a wavelength dependent fluorescence emission spectra, evident in **Figure 2**, where the excitation wavelength was varied from 425 nm to 525 nm in 25 nm increments. Previous HR–TEM analysis has shown that the technique itself adds limited information to the discussion of structural analysis of nano–carbon/organic hybrids as the organic species do not have a high contrast, limiting the ability of electron microscopy to see the structural details [4].

The structural porosity of the nano–carbon/organic hybrid samples can be exploited for sensing applications. In **Figure 3**, the quenching constants of the two different samples, DETA/CA and PEI_{1200}/CA, are shown at different excitation wavelengths, including λ_{ex} = 425 nm, 450 nm, 475 nm, 500 nm, and 525 nm. As expected, there is a wavelength dependence associated with the samples, possibly due to the change in quantum yield as a function of excitation wavelength. The samples were similar in their ability to sense DNT across multiple excitation wavelengths, with the PEI_{1200}/CA based system displaying slightly more sensitivity to DNT, which could be attributed to the emissive domains in PEI_{1200}/CA being somewhat larger with PEI_{1200} being much larger than DETA.

Sensing DNT at multiple wavelengths is important due to changing needs of a sensor and opens up possibilities for future sensor design. In **Figure 4** the quenching plots are shown for λ_{ex} = 425 nm, in both samples there is a downward curvature at lower concentrations of DNT. The slope over the entire range of data is 119 M^{-1} for DETA/CA and 123 M^{-1} for PEI_{1200}/CA. This effect is even more clearly seen when looking at lower concentration regions, in particular the range of 0.0 M to 1.0 x 10^{-4} M DNT, the slopes of the quenching plots are 513 M^{-1} for DETA/CA and 1012 M^{-1} for PEI_{1200}/CA. There is much larger variability in the quenching constants at this lower concentration. While the data is self–consistent such that the PEI_{1200}/CA has a larger constant, these values are high. The values suggest that there could be other factors at play such as a higher local quencher concentration that could be enabled by the structure of the nano–carbon/organic hybrids being porous. At longer excitation wavelengths, 450 nm – 525 nm, similar trends are observed. See **Table 1** for a summation of the data.

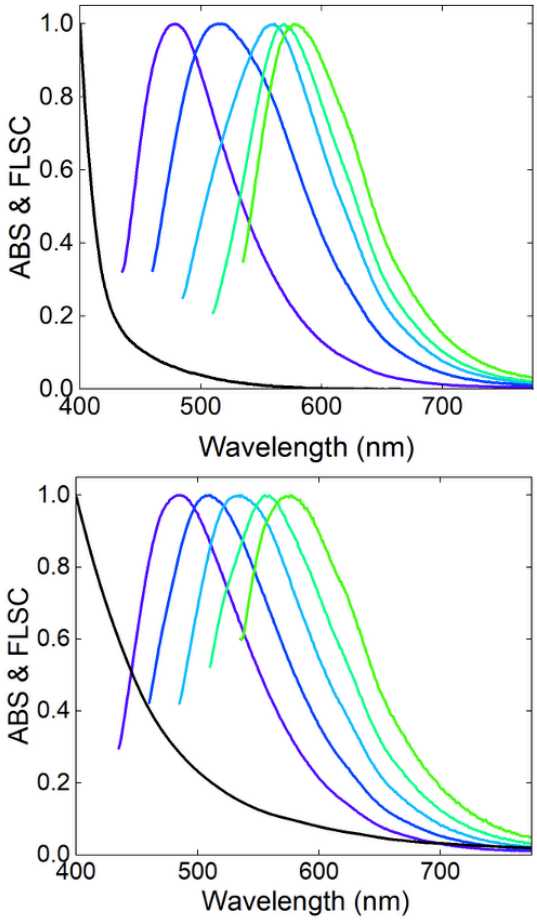


Figure 2. The absorption and fluorescence emission spectra of DETA/CA (top) and $PEI_{1200/}$CA (bottom).

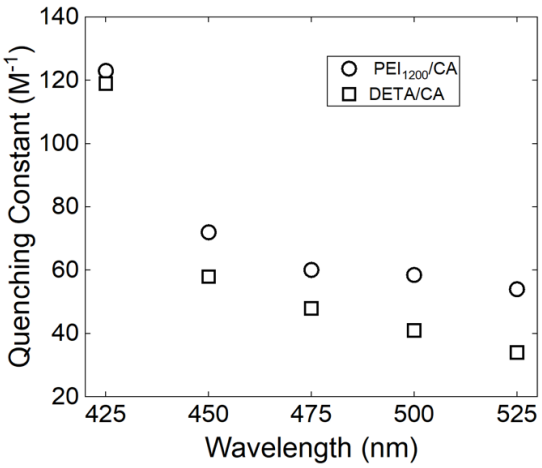


Figure 3. The excitation wavelength dependence of the quenching constants for DETA/CA and PEI_{1200}/CA.

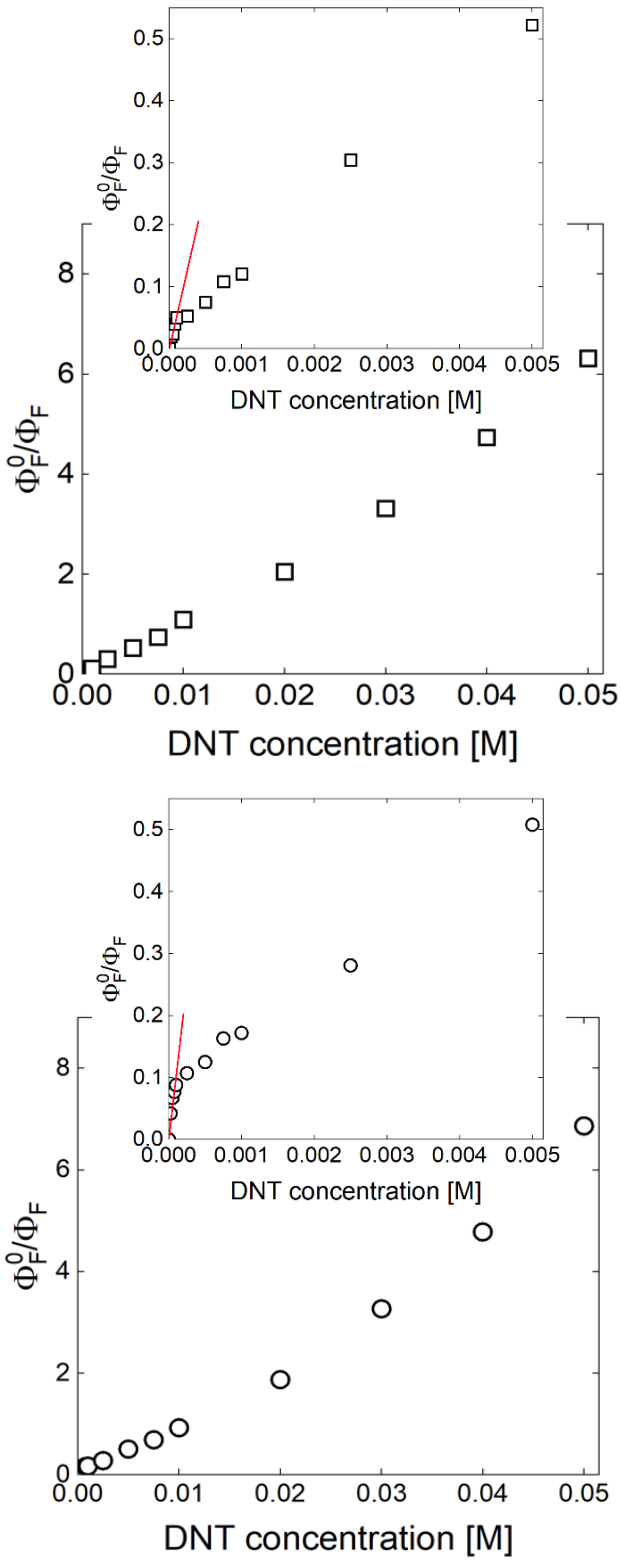


Figure 4. The quenching plots of DETA/CA (top) and PEI_{1200}/CA (bottom). The excitation wavelength used was 425 nm. Inset: the low DNT concentration region.

Carbon dots are known for their bright and colorful fluorescence in the visible spectrum and have been prepared with different organic species from PEG1500N, EDA, and PEI [1,2,15,29]. Using DETA in the synthesis of carbon nanomaterials has resulted in good optical properties, with fluorescence quantum yields greater than 12% at λ_{ex} = 425 nm. It is well understood that the quantum yield decreases with the excitation wavelength, as thoroughly discussed elsewhere [3]. The quenching plots for DETA/CA with λ_{ex} = 450 nm, 475 nm, 500 nm, and 525 nm are shown in **Figure 5**. When considering the total range (0.0 M to 5.0 x 10–2 M) of the quenching plot the quenching constant values as the wavelength increases are as follows: 59 M^{-1}, 48 M^{-1}, 41 M^{-1}, and 34 M^{-1}. Over the low concentration range (0.0 M to 1.0 x 10–4 M DNT) the values are high, again with increasing excitation wavelength from 450 nm to 525 nm the values are as follows: 240 M^{-1}, 558 M^{-1}, 324 M^{-1}, and 399 M^{-1}. Obviously, when incorporating the entire data range, the quenching constant decreases monotonically as the excitation wavelength increases. When analyzing the low concentration range the variability in quenching constants supports the notion that there is a local concentration effect or static quenching, namely quenching without the need for significant diffusion of the quenchers. Similar results were observed using PEI_{1200}/CA and are summarized in **Table 1**.

Despite their larger molecular weight, the PEI based system showed similar trends. In both PEI_{1200}/CA and DETA/CA samples (see **Figures 5** and **6**) the quenching plots may suggest higher local quencher concentrations. These results listed here are somewhat consistent with that of a classically defined carbon dot, such that there may be static quenching effects at low DNT concentrations [51,52], though the values reported here are an order of magnitude higher at lower DNT concentration. This increased sensitivity is beneficial for detecting hazardous materials at low concentrations.

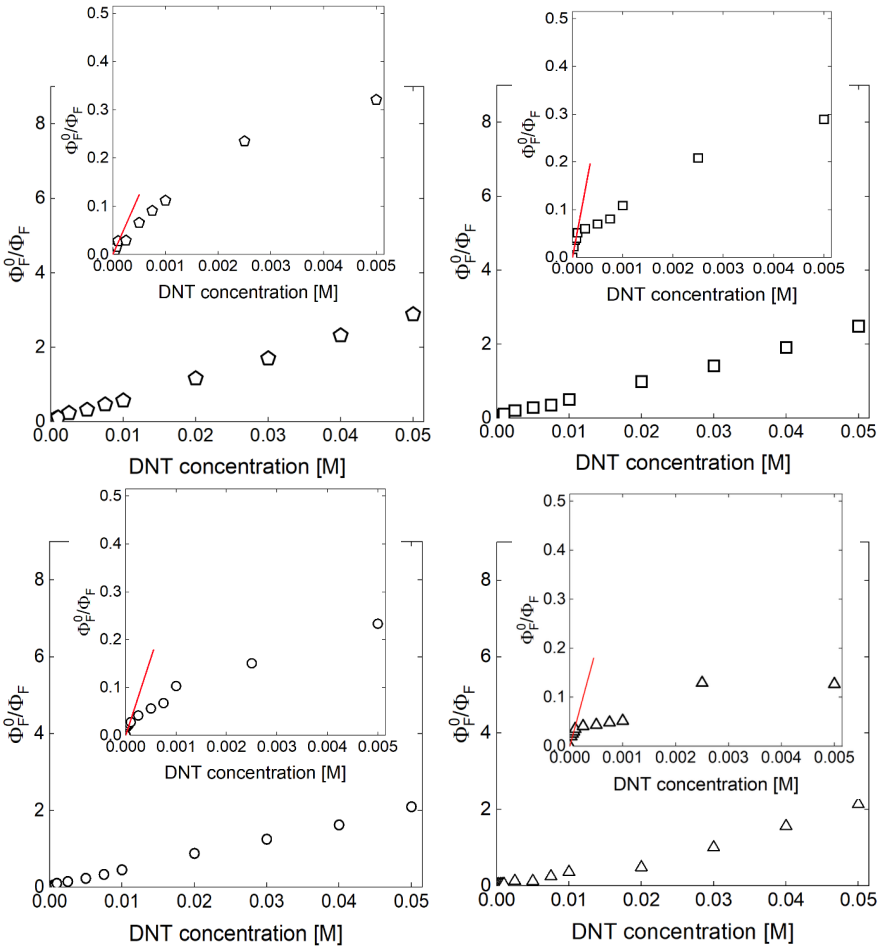


Figure 5. DETA/CA when excited at different wavelengths of 450 nm (pentagons), 475 nm (squares), 500 nm (circles), and 525 nm (triangles). The insets show the low concentration range of the quenching plot.

Table 1. The quenching constants of the two samples over different excitation wavelengths. The first value is the low concentration range (0.0 – 1.0 × 10^{-4} M DNT) and the second value is the given dataset (0.0 – 5.0 × 10^{-2} M).

	Quenching constants (M^{-1}) at low [DNT], at different λ_{ex} (nm)					**Quenching constants (M^{-1}) total dataset, at different λ_{ex} (nm)**				
Sample	425	450	475	500	525	425	450	475	500	525
DETA/CA	513	240	558	324	399	119	59	48	41	41
PEI_{1200}/CA	1012	584	564	328	840	123	72	60	58	54

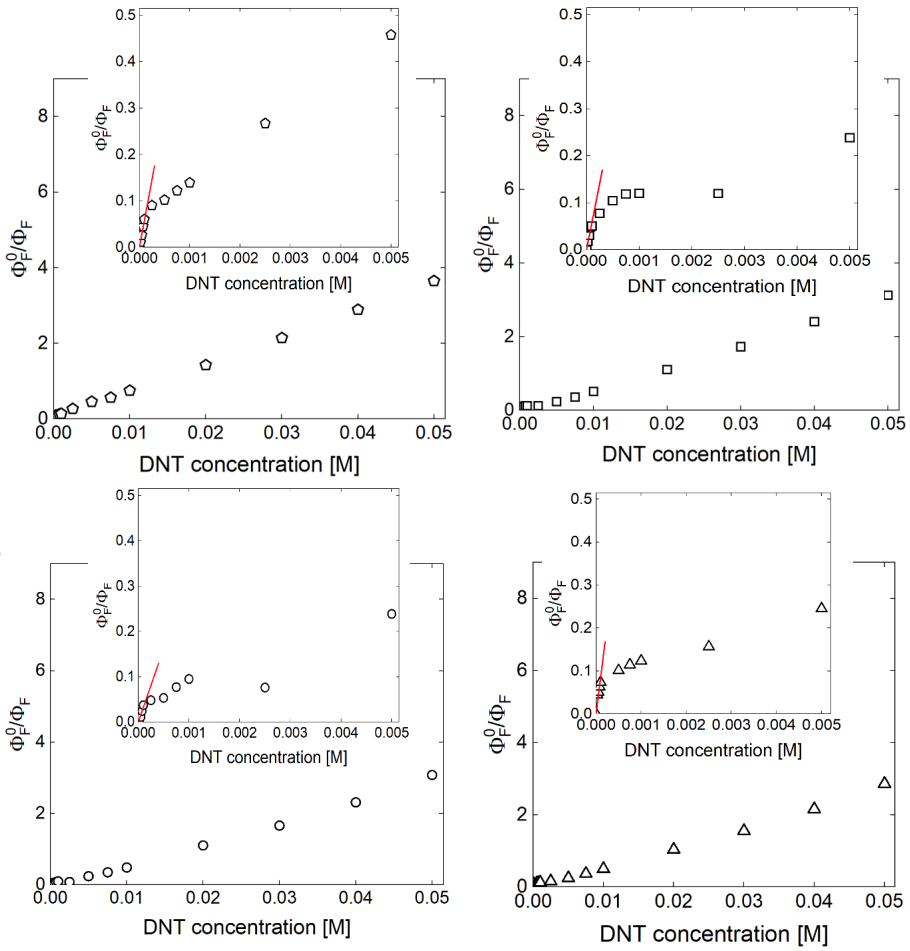


Figure 6. PEI_{1200}/CA when excited at different wavelengths of 450 nm (pentagons), 475 nm (squares), 500 nm (circles), and 525 nm (triangles). The insets show the low concentration range of the quenching plot.

The nano–carbon/organic hybrids are certainly interesting and can be sensitive to the presence of targeted analytes such as DNT. The relative fluorescence intensities of the DETA/CA and PEI_{1200}/CA shown in **Figures 7** and **8** suggest good sensitivity at low concentrations represented by the changes in fluorescence intensity. As the excitation wavelength increases there is a decrease in the quenching constant, likely attributed to the decrease in fluorescence quantum yield with the red–shift of the excitation wavelength. This excitation wavelength dependence has been seen in carbon nanomaterials dating back decades to early reports on carbon nanotubes [3,53,54]. In classically defined CDots it has been suggested that at lower concentrations, DNT sensing may have dynamic portions as well as static, but the clear steep slope shown in this report on the quenching plots at low concentration are indicative of other properties [2,52]. LeCroy et al. [52] showed

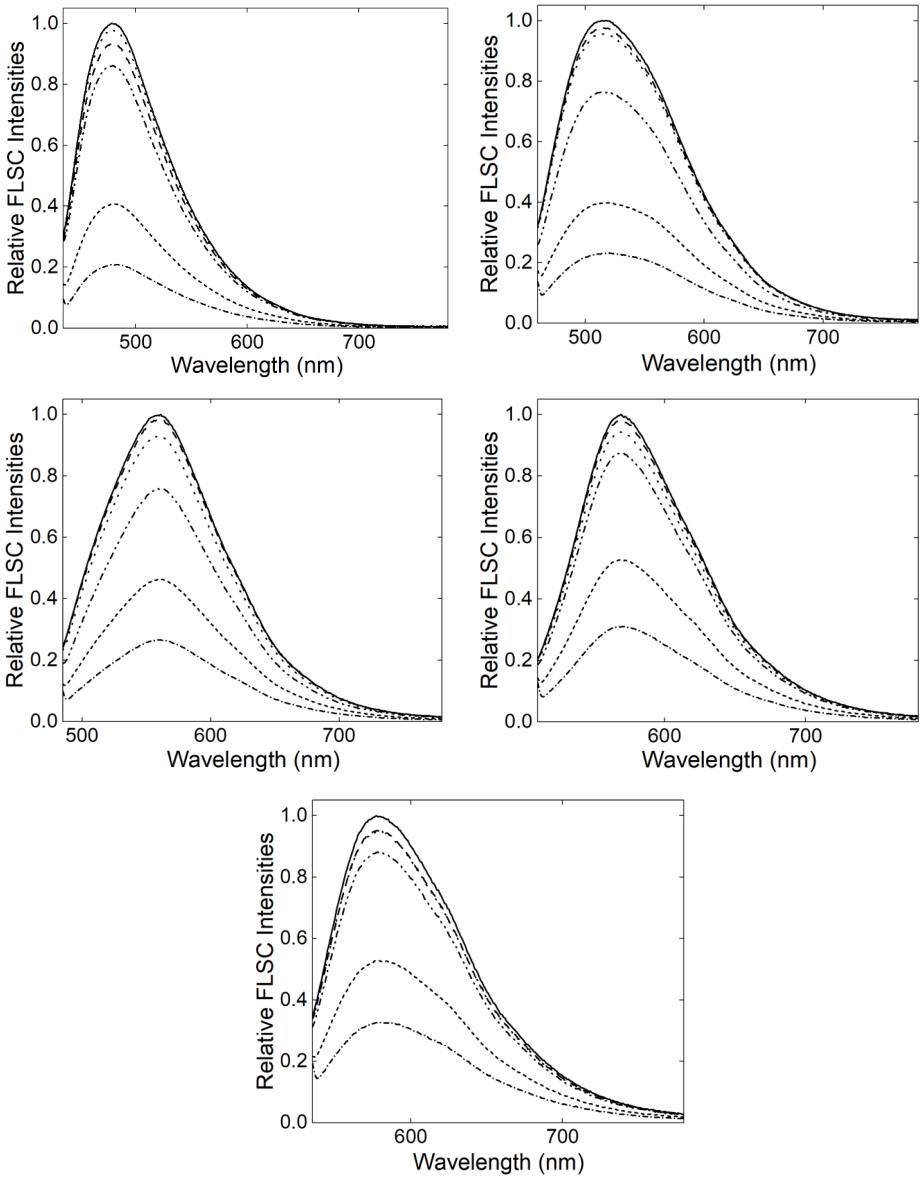


Figure 7. The DETA/CA fluorescence spectra at different concentrations when excited at 425 nm (top left), 450 nm (top right), 475 nm (middle left) and 500 nm (middle right) and 525 nm (bottom).

that EDA–CDots have static quenching effects, with some dynamic effects as well. In a comparison to EDA–CDots, the PEI_{1200}/CA system has quenching constants higher than those of EDA–CDots over the excitation wavelength range of 425 nm–475 nm. Wang et al. [29] observed similar phenomena as well in the fluorescence with Cu^{2+}. In that work [29], at lower concentrations the shapes of the quenching plots are incredibly steep and then curve downward as the Cu^{2+} concentration increases [29]. Herein, as the DNT concentration increases the same downward curvature is observed, and then as the concentration further increases the curvature turns upward. Static quenching could be a dominating factor here as the slope would suggest high quenching rate constants at lower DNT concentrations.

There has been a growing consensus in the research community related to the concern over processing conditions and looseness of the definition of a carbon dot [4,55,56]. While there may be some benefits from switching methodologies in the carbon dot synthesis, the effects may be balanced with less defined structural components [2,57–60]. This report suggests that there could be a trade-off that one could contend with

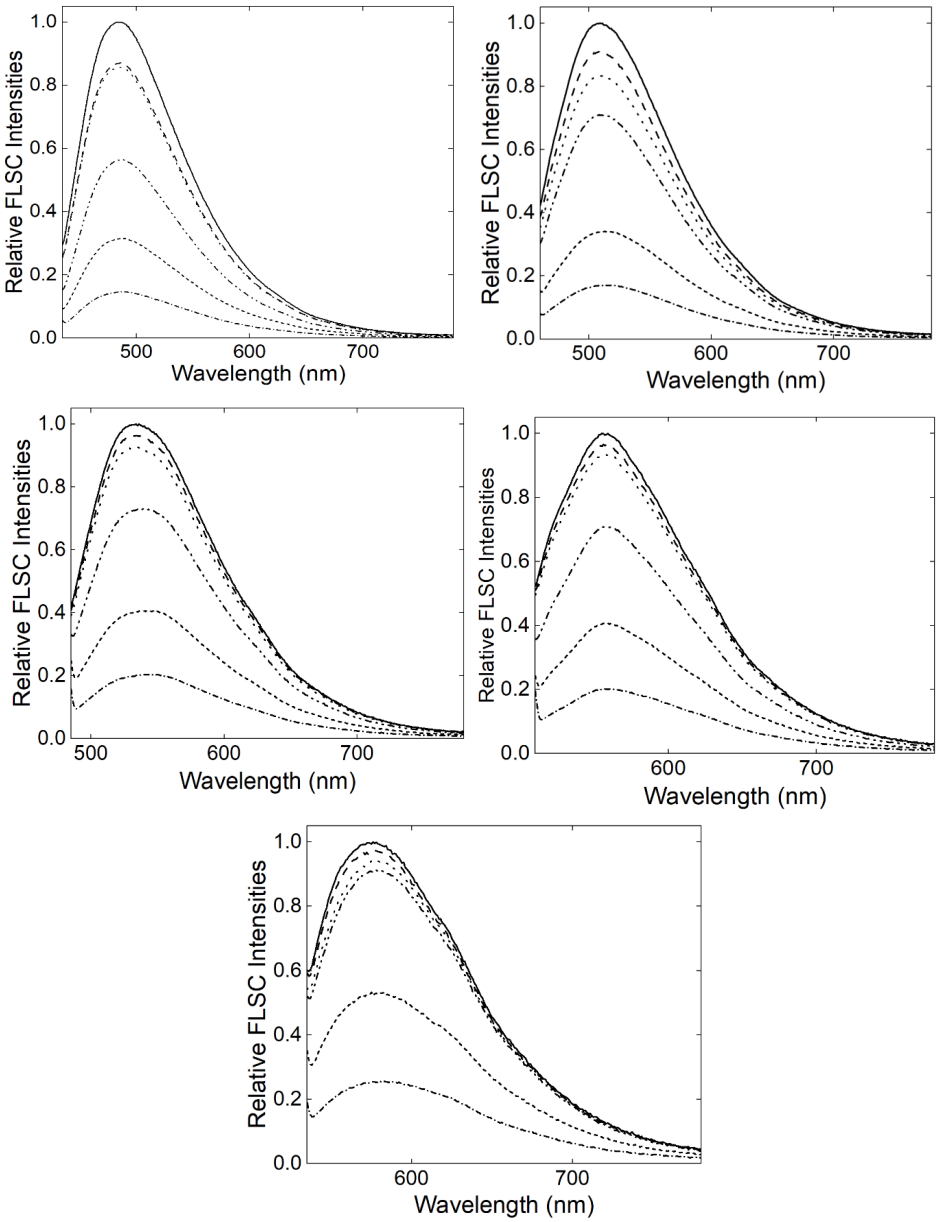


Figure 8. The PEI_{1200}/CA fluorescence spectra at different concentrations when excited at 425 nm (top left), 450 nm (top right), 475 nm (middle left), 500 nm (middle right) and 525 nm (bottom).

when building a carbon nanomaterial based fluorescence probe: cost effectiveness but lacking clearly defined structures thus complicating the analysis, or a more rigorous synthetic protocol that simplifies the analysis. As none of the starting materials are spectroscopically active at longer visible wavelengths, the nano–carbon domains in the nano–carbon/organic hybrids should be the source of the spectroscopic features. This highlights the ambiguity associated with this class of nanomaterials as there is no clear structural definition in comparison to classical CDots where there is a defined core with surface passivation. Finally, while some sensors built around CDot materials are cited for sensing ability at shorter wavelengths [61], this work provides interesting insights into these materials' sensing ability in the visible spectrum. Furthermore, using these longer wavelengths into the visible spectrum offers more opportunities for future sensor development as the probes mentioned here remain sensitive even at excitation wavelengths longer than 500 nm.

Conclusions

The high sensitivity of nano–carbon/organic hybrids for sensing 2,4–dinitrotoluene (DNT) was investigated and demonstrated. The large quenching constants observed over the lower DNT concentrations may arise from phenomena such as a higher local quencher concentration likely from the ability of amino moieties in the nano–carbon/organic hybrids to interact with DNT. Additionally, different excitation wavelengths were used for the systems showing good sensitivity across many different wavelengths in the visible spectrum from 425 nm–525 nm. The shared property of excitation wavelength dependent fluorescence emissions between these hybrid materials and classical CDots may be responsible for the similar trends at higher concentrations. However, the low concentration region tells a different story, such that the system is seemingly more sensitive to the quencher, which could be explained by a porous structure type. The divergence observed here from classical CDots certainly indicates that more rigorous and careful application of the carbon dot definition is warranted. While the presented nanomaterials are clearly capable of serving as a sensitive probe, careful use of language should be employed to prevent confusion of definitions.

Acknowledgements

K.S. was supported by an appointment to the Intelligence Community Postdoctoral Research Fellowship Program at Clemson University administered by Oak Ridge Institute for Science and Education (ORISE) through an interagency agreement between the U.S. Department of Energy and the Office of the Director of National Intelligence (ODNI). Y.–P.S. acknowledges financial support by the USDA grant (2023-67018-40681). J.C. was supported by a Graduate Research Fellowship sponsored by NASA through the South Carolina Space Grant Consortium.

Author Contributions

K.S.: conceptualization, investigation, writing, B.S.: investigation, S.D.: investigation, S.Y. investigation, J.C. investigation, Y.–P.S. conceptualization, writing.

Conflicts of Interest

The authors declare no conflicts of interest.

Data Availability Statement

Data available on request from the authors.

References

1. Sun YP, Zhou B, Lin Y, Wang W, Fernando KS, Pathak P, et al. Quantum-sized carbon dots for bright and colorful photoluminescence. Journal of the American Chemical Society. 2006 Jun 21;128(24):7756–7.
2. Ge L, Pan N, Jin J, Wang P, LeCroy GE, Liang W, et al. Systematic comparison of carbon dots from different preparations—consistent optical properties and photoinduced redox characteristics in visible spectrum and structural and mechanistic implications. J Phys Chem C. 2018 Aug 30;122(37):21667–76.
3. Sun YP. Carbon dots. Springer International Publishing; 2020.
4. Liang W, Sonkar SK, Saini D, Sheriff K, Singh B, Yang L, et al. Carbon Dots: Classically Defined versus Organic Hybrids on Shared Properties, Divergences, and Myths. Small. 2023 Aug;19(31):e2206680.
5. Rosso C, Filippini G, Prato M. Carbon dots as nano-organocatalysts for synthetic applications. ACS Catalysis. 2020 Jun 30;10(15):8090–105.
6. Iannazzo D, Celesti C, Cardo L, Prato M, Bitto A. Carbon dots for drug delivery: insights into their potential in nanopharmacology. Pharmacol Rev. 2025 Dec 9:100107.
7. Bartolomei B, Dosso J, Prato M. New trends in nonconventional carbon dot synthesis. Trends Chem. 2021 Nov 1;3(11):943–53.
8. Sheriff K, Liang W, Yerra S, Sulejmanovic D, Nelson C, Lupini A, et al. Carbon dots from surface-capping/passivation of small carbon nanoparticles with nanoscale titanium dioxide. Chemical Physics Letters. 2025 Apr 1;864:141913.
9. Luo PG , Sahu S , Yang ST , Sonkar SK , Wang J , Wang H , et al. Carbon "quantum" dots for optical bioimaging. J Mater Chem. 2013 Apr 28;1(16):2116–27.
10. Sun YP, Wang X, Lu F, Cao L, Meziani MJ, Luo PG, et al. Doped Carbon Nanoparticles as a New Platform for Highly Photoluminescent Dots. J Phys Chem C. 2008 Nov 27;112(47):18295–8.
11. Anilkumar P, Wang X, Cao L, Sahu S, Liu JH, Wang P, Korch K, Tackett KN 2nd, Parenzan A, Sun YP. Toward quantitatively fluorescent carbon-based "quantum" dots. Nanoscale. 2011 May;3(5):2023–7.
12. Wang X, Cao L, Yang ST, Lu F, Meziani MJ, Tian L, et al. Bandgap-like strong fluorescence in functionalized carbon nanoparticles. Angew Chem. 2010 Jul 19;49(31):5310–4.
13. Sciortino A, Cayuela A, Soriano ML, Gelardi FM, Cannas M, Valcárcel M, et al. Different natures of surface electronic transitions of carbon nanoparticles. Phys Chem Chem Phys. 2017 Aug 30;19(34):22670–7.
14. Sciortino A, Ferrante F, Mauro N, Buscarino G, Sciortino L, Giammona G, et al. Disclosing the emissive surface traps in green-emitting carbon nanodots. Carbon. 2021 Mar 1;173:454–61.
15. LeCroy GE, Messina F, Sciortino A, Bunker CE, Wang P, Fernando KS, et al. Characteristic excitation wavelength dependence of fluorescence emissions in carbon "quantum" dots. J Phys Chem C. 2017 Dec 21;121(50):28180–6.

16. Gonçalves H, Jorge PA, Fernandes JR, da Silva JC. Hg (II) sensing based on functionalized carbon dots obtained by direct laser ablation. Sens Actuators B: Chem. 2010 Mar 19;145(2):702–7.

17. Tripathi KM, Sonker AK, Sonkar SK, Sarkar S. Pollutant soot of diesel engine exhaust transformed to carbon dots for multicoloured imaging of E. coli and sensing cholesterol. RSC Adv. 2014 Jul 10;4(57):30100–7.

18. Thulasi S, Kathiravan A, Asha Jhonsi M. Fluorescent carbon dots derived from vehicle exhaust soot and sensing of tartrazine in soft drinks. ACS Omega. 2020 Mar 31;5(12):7025–31.

19. Mandal T, Mishra SR, Singh K, Agarwalla H, Masto RE, Kumar M, et al.Fluorescent carbon nanomaterials from coal and its derivatives: structure, properties, and applications. J Nanoparticle Res. 2023 Jun;25(6):125.

20. Ghosh T, Ghosh R, Basak U, Majumdar S, Ball R, Mandal D, Et al. Candle soot derived carbon nanodot/polyaniline hybrid materials through controlled grafting of polyaniline chains for supercapacitors J Mater Chem A. 2018 Apr 17;6(15):6476–92.

21. Kaur P, Chopra L, Pal K, de Souza Jr FG, Kralj S, Oluwafemi SO, et al. Guava leaf-derived carbon quantum dots as fluorescent probes for turn-on/off detection of Ba2+, Pb2+, Sn2+, and Hg2+ ions. Ceram Int. 2025 Jul 31;51:47202–17.

22. Chatzimarkou A, Chatzimitakos TG, Kasouni A, Sygellou L, Avgeropoulos A, Stalikas CD. Selective FRET-based sensing of 4-nitrophenol and cell imaging capitalizing on the fluorescent properties of carbon nanodots from apple seeds. Sens Actuators B: Chem. 2018 Apr 1;258:1152–60.

23. Zhang J, Chu S, Tao C, Yan J, Jiang Y, Lu Y. Nitrogen-doped carbon dots as efficient turn-on fluorescent probe for assay of organophosphorus pesticides. Chem Phys Mater. 2024 Oct 1;3(4):462–9.

24. Deng X, Yang H, Gong AJ, Huang XM, Li L. Sensitive and selective chemosensor for Fe3+ detection using carbon dots synthesized by microwave method. Spectrochim. Acta A. 2025 Jun 5;334: 125907.

25. Annamalai A, Elumalai S, Sangaraju S, Hassan FM. Bottom-up microwave transformation of molecules to carbon dots for detection and encryption applications. RSC Adv. 2026 Jan 21;16(5):4618–28.

26. Khan S, Sharma A, Ghoshal S, Jain S, Hazra MK, Nandi CK. Small molecular organic nanocrystals resemble carbon nanodots in terms of their properties. Chem Sci. 2017 Dec 20;9(1):175–80.

27. Shi L, Yang JH, Zeng HB, Chen YM, Yang SC, Wu C, et al. Carbon dots with high fluorescence quantum yield: the fluorescence originates from organic fluorophores. Nanoscale. 2016 Jul 28;8(30):14374–8.

28. Liu X, Li HB, Shi L, Meng X, Wang Y, Chen X, et al. Structure and photoluminescence evolution of nanodots during pyrolysis of citric acid: from molecular nanoclusters to carbogenic nanoparticles. J Mater Chem C. 2017 Oct 12;5(39):10302-12.

29. Wang P, Meziani MJ, Fu Y, Bunker CE, Hou X, Yang L, et al. Carbon dots versus nano-carbon/organic hybrids–dramatically different behaviors in fluorescence sensing of metal cations with structural and mechanistic implications. Nanoscale Adv. 2021 Apr 20;3(8):2316–24.

30. Garg R, Anjum F, Salam A, Kaushik K, Sharma S, Sahrawat U, et al. Tracking the super resolved structure of mitochondria using red emissive carbon nanodots as a fluorescent biomarker. Chem. Commun. 2023 Nov 9;59(90):13454–7.

31. Cao L, Wang X, Meziani MJ, Lu F, Wang H, Luo PG, et al. Carbon dots for multiphoton bioimaging. J Am Chem Soc. 2007 Sep 19;129(37):11318–9.

32. Sturabotti E, Sierra-Serrano B, Apresto SM, Cesco M, Comparini L, Cardo L, et al. Carbon dots as multi-modal contrast agents: opportunities and open challenges for in vivo bioimaging. Adv Drug Deliv Rev. 2025 Sep;224:115659.

33. Wang J, Sahu S, Sonkar SK, Tackett II KN, Sun KW, Liu Y, et al. Versatility with carbon dots–from overcooked BBQ to brightly fluorescent agents and photocatalysts. RSC Advances. 2013 Aug 19;3(36):15604–7.

34. Zhang B, Maimaiti H, Zhang DD, Xu B, Wei M. Preparation of coal-based C-Dots/TiO2 and its visible-light photocatalytic characteristics for degradation of pulping black liquor. J Photochem Photobiol A Chem. 2017 Aug 1;345:54–62.

35. Wang X, Cao L, Lu F, Meziani MJ, Li H, Qi G, et al. Photoinduced electron transfers with carbon dots. Chem Commun (Camb). 2009 Jul 7;(25):3774–6.

36. Sarkar PK, Kar P, Halder A, Lemmens P, Pal SK. Development of highly efficient dual sensor based on carbon dots for direct estimation of iron and fluoride ions in drinking water. ChemistrySelect. 2019 Apr 24;4(15):4462–71.

37. Roy S. Detection of fluoride ion by carbon dots-based fluorescent probes. J Mol Struct. 2025 Jan 5;1319:139465.

38. Xiang Q, Geng W, Guo X, Liu Y, Liu S, Jin X, et al. A dual quantum dots-based ratio fluorescent probe for detecting Glyphosate in agricultural products. Microchem J. 2025 May 1;212:113214.

39. Tian X, Peng H, Li Y, Yang C, Zhou Z, Wang Y. Highly sensitive and selective paper sensor based on carbon quantum dots for visual detection of TNT residues in groundwater. Sens Actuators B Chem. 2017 May 1;243:1002–9.

40. Bruno F, Sciortino A, Buscarino G, Soriano ML, Ríos Á, Cannas M, et al. A Comparative Study of Top-Down and Bottom-Up Carbon Nanodots and Their Interaction with Mercury Ions. Nanomaterials (Basel). 2021 May 12;11(5):1265.

41. Wang J, Wei J, Su S, Qiu J. Novel fluorescence resonance energy transfer optical sensors for vitamin B12 detection using thermally reduced carbon dots. New J Chem. 2014 Dec 16;39(1):501–7.

42. Bruno F, Sciortino A, Buscarino G, Cannas M, Gelardi FM, Messina F, et al. Sensing of transition metals by top-down carbon dots. Appl Sci. 2021 Nov 4;11(21):10360.

43. Santonocito R, Intravaia M, Caruso IM, Pappalardo A, Trusso Sfrazzetto G, et al. Fluorescence sensing by carbon nanoparticles. Nanoscale Adv. 2022 Apr 12;4(8):1926–48.

44. Jamil AK, Sivanesan A, Izake EL, Ayoko GA, Fredericks PM. Molecular recognition of 2, 4, 6-trinitrotoluene by 6-aminohexanethiol and surface-enhanced Raman scattering sensor. Sens Actuators B Chem. 2015 Dec 31;221:273–80.

45. Ferrari C, Attolini G, Bosi M, Frigeri C, Frigeri P, Gombia E, et al. Detection of Nitroaromatic Explosives in Air by Amino-Functionalized Carbon Nanotubes. Nanomaterials (Basel). 2022 Apr 8;12(8):1278.

46. Singh B, Adcock AF, Dumra S, Collins J, Yang L, Bunker CE, et al. Microwave-Assisted Carbonization Processing for Carbon Dot-like Nanomaterials with Antimicrobial Properties. InMicro 2025 Mar 17;5(1):14.

47. Hou X, Hu Y, Wang P, Yang L, Al Awak MM, Tang Y, et al. Modified Facile Synthesis for Quantitatively Fluorescent Carbon Dots. Carbon N Y. 2017 Oct;122:389–94.

48. Zhu H, Wang X, Li Y, Wang Z, Yang F, Yang X. Microwave synthesis of fluorescent carbon nanoparticles with electrochemiluminescence properties. Chem Commun (Camb). 2009 Sep 14;(34):5118–20.

49. Wang X, Qu K, Xu B, Ren J, Qu X. Microwave assisted one-step green synthesis of cell-permeable multicolor photoluminescent carbon dots without surface passivation reagents. J Mater Chem. 2011 Feb 8;21(8):2445–50.

50. Jaiswal A, Ghosh SS, Chattopadhyay A. One step synthesis of C-dots by microwave mediated caramelization of poly(ethylene glycol). Chem Commun (Camb). 2012 Jan 11;48(3):407–9.

51. Lakowicz JR, editor. Principles of fluorescence spectroscopy. Boston, MA: Springer US; 2006.

52. LeCroy GE, Fernando KS, Bunker CE, Wang P, Tomlinson N, Sun YP. Steady-state and time-resolved fluorescence studies on interactions of carbon "quantum" dots with nitrotoluenes. Inorganica Chim Acta. 2017 Nov 1;468:300–7.

53. Kose ME, Harruff BA, Lin Y, Veca LM, Lu F, Sun YP. Efficient quenching of photoluminescence from functionalized single-walled carbon nanotubes by nitroaromatic molecules. J Phys Chem B. 2006 Jul 27;110(29):14032–4.

54. Banerjee S, Wong SS. Structural characterization, optical properties, and improved solubility of carbon nanotubes functionalized with Wilkinson's catalyst. J Am Chem Soc. 2002 Jul 31;124(30):8940–8.

55. Song Y, Zhu S, Zhang S, Fu Y, Wang L, Zhao X, et al. Investigation from chemical structure to photoluminescent mechanism: a type of carbon dots from the pyrolysis of citric acid and an amine. Journal of Materials Chemistry C. 2015 Jun 4;3(23):5976–84.

56. Michaud V , Pracht J , Schilfarth F , Damm C , Platzer B , Haines P , et al . Well-separated water-soluble carbon dots via gradient chromatography. Nanoscale. 2021 Aug 14;13(30):13116–28.

57. Desalegn YM, Chen D, Han Y, Yu J, An H, Liu P, et al. Harnessing Carbon Dots for Photocatalytic Energy Conversion: Challenges and Opportunities. Small. 2026 Jan;22(5):e09184.

58. Schneider J, Reckmeier CJ, Xiong Y, von Seckendorff M, Susha AS, Kasák P, et al. Molecular fluorescence in citric acid-based carbon dots. The Journal of Physical Chemistry C. 2017 Jan 26;121(3):2014–22.

59. Hinterberger V , Damm C , Haines P , Guldi DM , Peukert W . Purification and structural elucidation of carbon dots by column chromatography. Nanoscale. 2019 Apr 25;11(17):8464–74.

60. Ali MH, Janesko BG, Rana MM, Saleem U, Gajula NM. Benchmarking a Computational Workflow Modeling Near-Infrared-Emitting Graphene Quantum Dots. The Journal of Physical Chemistry C. 2026 Mar 19;130(13):4800–13.

61. Jia R, Guo J, Li H, Zhang L, Wu X. Highly efficient N-doped carbon dots for ultrasensitive and selective detection of picric acid in explosive residues. Spectrochim Acta A Mol Biomol Spectrosc. 2026 Feb 15;347:126896.